Prediction of Oxidation Assisted Crack Growth Behavior within Hot Section Gas Turbine Components

Graham Webb, Tom Strangman, Norm Frani, Chet Daté, Lloyd Wilson and Rajiv Rana
AlliedSignal Engines
111 S. 34th Street
Phoenix, Arizona 85072-2181 USA

Dennis Fox
NASA-Lewis Research Center
21000 Brookpark Road
Cleveland, Ohio 44135 USA

ABSTRACT

This paper presents a physically-based deterministic methodology for prediction of the crack growth resistance of superalloys within gas turbine engine environments. The model combines experimentally determined temperature and pressure dependent superalloy oxidation rates with crack growth rates obtained from thermal-mechanical fatigue (TMF) specimen testing to develop a crack growth rate law for oxidation assisted crack growth behavior. This information is then used in conjunction with standard linear elastic fracture mechanics (LEFM) methods to predict propagation lives. The propagation analysis procedure is combined with previously presented procedures for the prediction of coating cracking during TMF loading (Strangman [1]). The combination results in an initiation plus propagation lifing strategy for superalloy gas turbine components subjected to thermal-mechanical fatigue. This analytical procedure has been found to predict the measured crack sizes obtained from superalloy components after engine testing with acceptable accuracy.

INTRODUCTION

Thermal Mechanical Fatigue (TMF) cracking of hot section gas turbine components remains a significant barrier to the establishment of long term gas turbine engine component durability. Cracking is most frequently observed on high cost superalloy precision cast airfoil components (i.e. blades and vanes), and usually results from initial cracking of the environmentally resistant airfoil coatings [2-5]. Once initiated, these cracks can propagate into the underlying superalloy substrate as a result of environmentally assisted fatigue crack propagation. The current work presents experimental and analytical methods for prediction of such behavior under the influence of an open loop out-of-phase TMF load cycle wherein a compressive strain hold is imposed (e.g. Figure 1), such cycles being representative of the time dependent response of turbine airfoil surfaces. Such waveforms are observed to result in cracking and subsequent retirement of gas turbine airfoil components. In previous work, a procedure was developed and presented for the prediction of coating cracking during out-of-phase TMF cycling [1]. In this investigation, the ductility, creep resistance, and thermal expansion mismatch between coating and substrate were found to determine the coating's resistance to cracking during out-of-phase TMF cycling. These variables were then used to estimate coating stresses resulting from the imposed strain cycle. Due to its extremely low creep resistance, the environmentally protective intermetallic coating experiences significant stress relaxation in the TMF critical airfoil locations which experience compressive thermal strains while operating. This phenomena shifts the cyclic mean stress, resulting in the development of tensile stresses within the coating (Figure 2). These stresses, if of sufficient magnitude, can subsequently overload (or fatigue) the coating material resulting in the formation of coating cracks. Once present, coating cracks are observed to propagate into the underlying substrate during further engine cycling as a result of environmentally assisted crack growth (Figure 3).

Metallurgical examination of such cracks (Figure 4) reveals severe oxidation of the crack faces due to the exposure of bare substrate material to the high temperature/pressure turbine environment. More importantly, oxidation is also observed to affect the material directly ahead of the growing crack tip (hereon termed "process zone", Figure 5). This phenomena will obviously modify the superalloy's intrinsic resistance to crack growth, and thus TMF crack propagation is observed to involve environmental, as well as mechanical crack growth mechanisms. As will be demonstrated, this environmental damage mode can dominate the crack growth process at the high temperatures and pressures typical of the gas turbine engine environment. Physical descriptions which ignore crack tip oxidation are shown to result

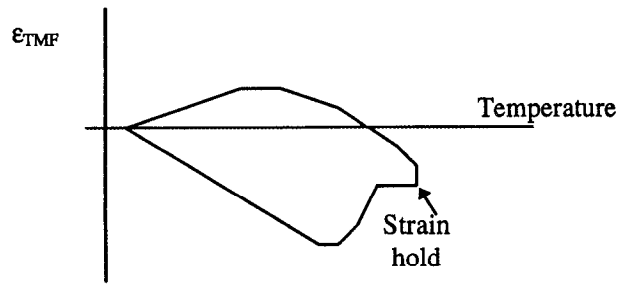

Figure 1. Schematic representation of an open loop out-of-phase thermal-mechanical fatigue strain cycle with a compressive strain hold.

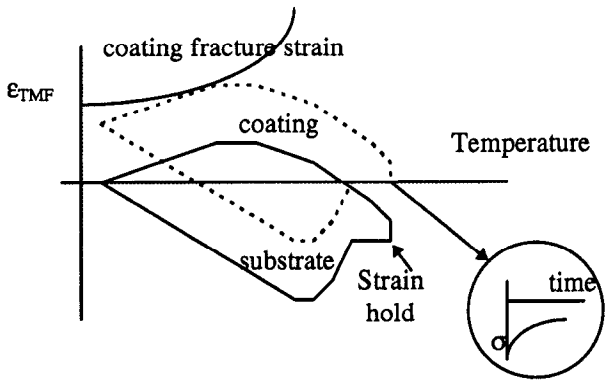

Figure 2. Schematic representation for the development of tensile coating cracks during TMF cycling of the underlying substrate material.

Superalloys 1996
Edited by R. D. Kissinger, D. J. Deye, D. L. Anton,
A. D. Cetel, M. V. Nathal, T. M. Pollock, and D. A. Woodford
The Minerals, Metals & Materials Society, 1996

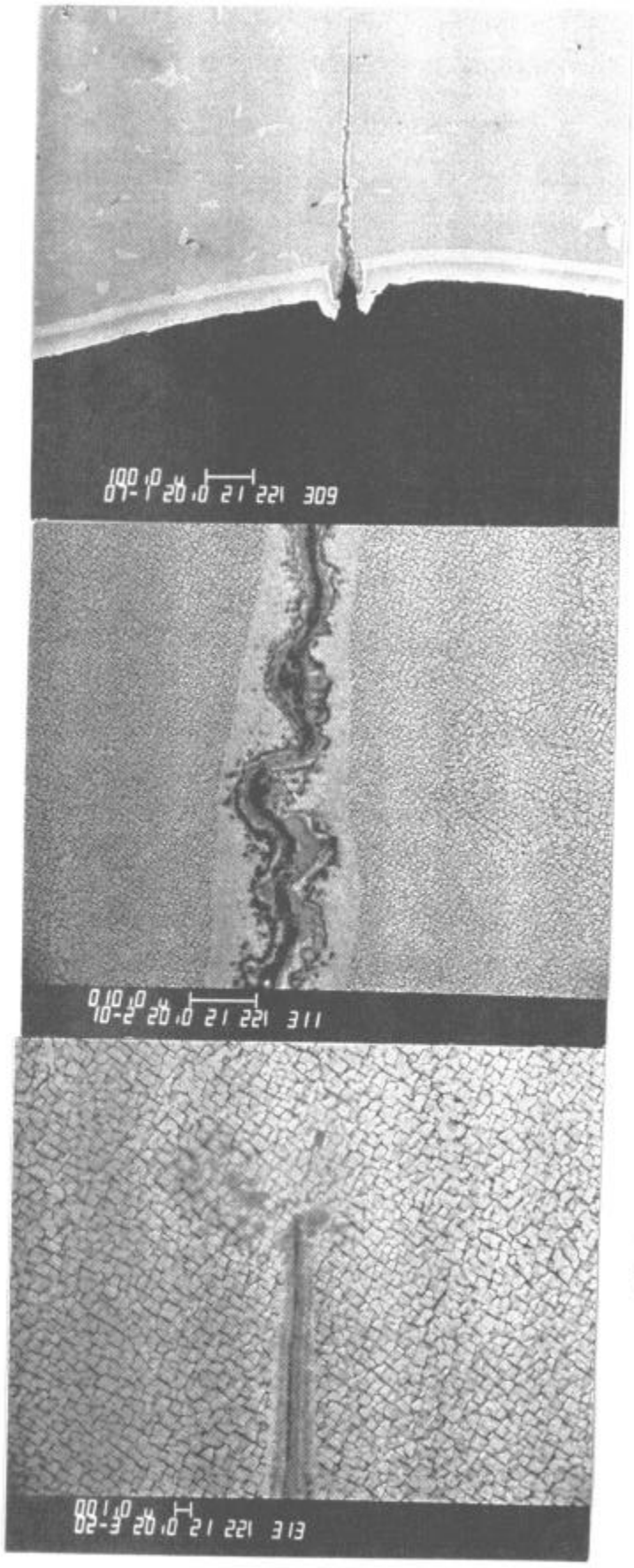

Figure 3. Coating initiated cracking of a CMSX-3 gas turbine airfoil component after experiencing open loop out-of-phase TMF cycling. Coating cracks are observed to propagate into the superalloy substrate as a result of environmentally assisted fatigue crack growth.

Figure 4. Oxidation of CMSX-3 crack faces during TMF cycling. Note depletion of gamma prime phase adjacent to crack surfaces.

Figure 5. Oxidation affected crack tip process zone observed within CMSX-3 gas turbine airfoil component after experiencing turbine thermal cycling.

Table I. Compositions ranges (in wt%) of Ni-base superalloys tested

Alloy	Ni	Al	Ti	Cr	Co	Ta	W	Mo	Hf	Cb	Re	B	C	Zr
IN738LC	bal.	3.2-3.7	3.2-3.7	15.7-16.3	8.0-9.0	1.5-2.0	2.4-2.8	1.5-2.0	-	0.6-1.1	-	0.007-0.012	0.09-0.13	0.03-0.08
MarM 247	bal.	5.3-5.7	0.9-1.2	8.0-8.3	9.0-11.0	2.8-3.3	9.5-10.5	0.5-0.8	1.20-1.60	-	-	0.01-0.02	0.13-0.17	0.03-0.08
CMSX3	bal.	5.5-5.8	0.8-1.2	7.2-8.2	4.3-4.9	5.8-6.2	7.6-8.4	0.3-0.7	0.07-0.15	-	-	0.003 max	0.02 max	0.008 max
SC180	bal.	5.0-5.4	0.9-1.1	5.0-6.0	9.7-10.3	8.0-9.0	4.8-5.2	1.4-2.0	0.08-0.12	-	2.8-3.2	0.002 max	0.02 max	0.008 max

in anti-conservative estimates of superalloy crack growth resistance, particularly for short cracks (high aspect ratio shallow cracks).

Although widely recognized [6], very little experimental data has been generated within the open literature to describe this phenomena, or its effect on TMF crack growth during cycling of gas turbine engine components. Much of this may be attributed to the experimental difficulty of conducting material crack growth measurements under high temperature and high pressure environments, in addition to the waveform specific nature of this phenomena. Recognizing this current deficiency, the current experimental work was conducted with the goal of providing a methodology to capture the primary factors influencing superalloy degradation during gas turbine airfoil TMF cycles using basic laboratory measurements. Towards this end experiments have been conducted to estimate both environmental and mechanical TMF crack growth components. Environmental crack growth is predicted upon the basis of experiments which evaluate superalloy oxidation rates as a function of temperature and oxygen activity (pressure). This information is then used to create a model for defining the environmental crack growth law.

Once defined, the environmental crack growth is analytically combined with measured values of the substrate materials crack growth resistance during out-of-phase TMF crack growth rate experiments at various temperatures and stress R-ratios. Such experiments, conducted using simple triangle out-of-phase waveforms in which minimum and maximum loads are cycled out-of-phase of temperature, estimate the superalloy's resistance to mechanical crack growth. Upon definition of the operating environment (temperatures, pressures, and time sequencing) it is possible to estimate a waveform dependent crack growth rate law specifically applicable to the case under analysis. This crack growth resistance is subsequently combined with a numerically simulated or assumed crack scenario to calculate the component TMF crack propagation life for an envisioned (or known) failure scenario. When combined with the predicted coating crack initiation life, component TMF life predictions are created.

The following description shall define the experimental and analytical procedures used to create the above component TMF lifing methodology applicable for superalloys used to manufacture airfoils within the hot section of gas turbine engines.

Experimental Procedures and Results

Determination of Environmental TMF Crack Growth Rates

As described in the previous section, model environmental crack growth laws were created using measured rates of superalloy oxidation under both transient (i.e. linear) and steady state conditions as a function of temperature and oxygen pressure. When initially exposed to a high temperature oxygen containing environment, all of the metallic elements in the alloy can be converted to their oxides. Initially NiO and low density spinels are the fastest forming oxides and scale growth is linear with respect to time. As the transient oxide scale thickens, the oxygen activity at the metal interface decreases, permitting chromia and other more thermodynamically stable oxides (e.g. Al_2O_3 and HfO_2) to accumulate. As these dense adherent oxides grow under and through the initial oxide layer, the oxidation kinetics become limited by the rate of diffusion of oxygen and aluminum and/or chromium and parabolic growth kinetics become established in which the oxide scale grows proportional to the square root of time.

Thus, when un-cracked, the initial transient oxide scale results in the formation of a more protective oxide scale and the rate of oxidation decreases. However, the oxide scale does not remain un-cracked in the process zone ahead of a growing TMF crack. The low toughness transient oxide scale is assumed to rupture during every engine cycle exposing fresh metal which re-establishes the transient (i.e. linear) rate of oxidation at the crack tip. For this reason it is reasonable to assume that the rate of environmental crack growth is proportional to the rate of oxidation of the superalloy material for the turbine operating environment (i.e. temperatures/pressures). Due to this, experiments were conducted to measure the rate of oxide scale growth for a variety of superalloy materials (Table I) during both transient and parabolic oxidation. Oxidation kinetics were estimated from weight change experiments for specimens of known surface area. Although only oxidation data for CMSX-3 will be utilized further within the current paper, the information from all alloys tested is also provided to permit dissemination of this information within the public domain.

All samples were ground to 600 grit using SiC abrasive paper. Specimens were cleaned with detergent, distilled water, acetone, and ethyl alcohol. Oxidation experiments were conducted in a vertical tube furnace at 800°, 900°, 1000°, 1100°, and 1200°C. Quartz furnace tubes with an internal diameter of 2.2 cm were used. Samples were suspended from a sapphire hook. The oxidation kinetics were measured using thermogravimetric analysis (TGA). Sample weight change was continuously measured throughout the experiment using a recording microbalance. Exposure time for each sample was six hours. The furnace environment was either ambient air or high purity oxygen maintained at a gas flow rate of 100 cm^2/min, corresponding to a velocity of 0.44 cm/sec. Samples were suspended in the tube furnace in the air, or flowing gas environment. Temperature was instantaneously applied to the specimens by raising the heated furnace around the sample. The experimental data obtained from these experiments reveals that the rate of superalloy oxidation is linear with respect to time for several minutes, and then slows to the more protective parabolic oxidation rate. Although limited, this data suggests that the transition time from linear to parabolic rate kinetics exhibits a baseline value of 0.17 hours in stagnant air. Transient (i.e. linear) oxidation rates are further found to be strongly dependent upon the activity of gaseous oxygen present within the tube furnace (Figure 6). In contrast, parabolic oxidation rates are observed to be independent of oxygen pressure. The temperature dependence of the linear and parabolic oxidation rates for the four superalloys are presented within Figure 7. Fitting of an Arrenhius-type kinetic equation to the experimental data results in the following equations for the linear and parabolic oxidation rate constants:

$$\Re_{linear} = \sqrt{P}\,\beta_{linear}\exp(-Q_{linear}/kT) \quad (1)$$

and

$$\Re_{parabolic} = \beta_{parabolic}\exp(-Q_{parabolic}/kT) \quad (2)$$

where: $\Re_{linear}$, $\Re_{parabolic}$ are the rate constants in mg/cm^2/hr and mg/cm^2/$hr^{1/2}$

β's are substrate dependent linear (transient) and parabolic (steady state) intercepts

Q's are substrate dependent linear and parabolic activation energies

k is Boltzmann's constant

T is the crack tip metal temperature (°K)

P is the turbine operating pressure (atm)

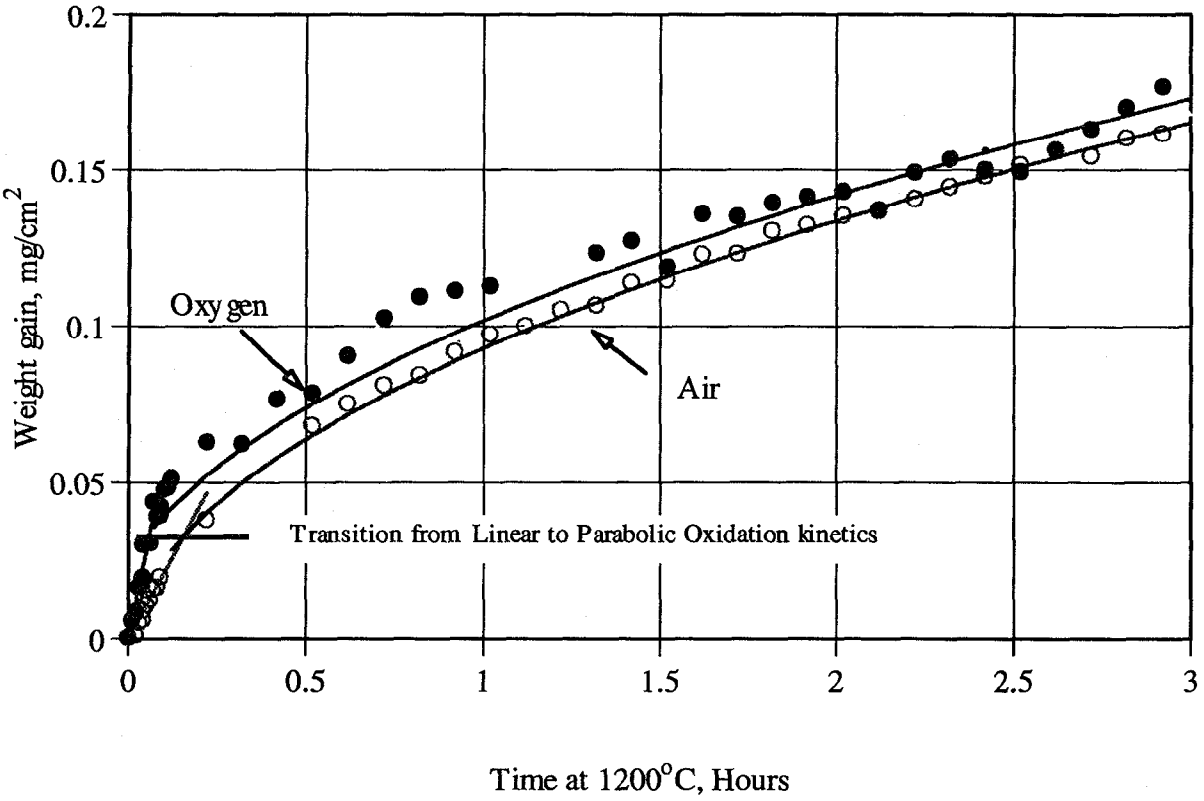

Figure 6. Effect of oxygen activity on transient and steady state oxidation of CMSX-3 at 1200°.

These equations describe the kinetics for weight gain in mg/cm^2 of exposed surface area, which may be analytically transformed into an equivalent environmentally degraded crack tip process zone. This is accomplished by determining the volume change associated with a weight gain of 1 mg/cm^2. For the CMSX-3 alloy, the conversion of the individual elements to their oxides results in a calculated scale thickness of 3.56 μm. Using this calculated value, the environmental crack propagation is obtained by assuming that the oxide layer forming at the crack tip process zone is completely cracked upon completion of the TMF cycle. These methods form the basis for the environmental crack growth rate law used within the analytical formulation.

Determination of TMF Mechanical Crack Growth Rates

Crack growth rate measurements of the single crystal superalloy CMSX-3 were conducted for an experimental 538°-982° C triangle out-of-phase waveform cycle. CMSX-3 test material was cast, HIPped, and heat treated in the form of 12.2 mm diameter bars nominally 152.4 mm in length in which the primary [001] crystallographic axis is within 10° of the bar longitudinal axis as verified by Laue back reflection method. Secondary crystallographic orientations were also determined. After casting the bars were HIPped at 1300°C at 100 MPa, cooled, then solutioned at 1200°C for 4 hours followed by forced cooling (>55° C/min to below 982°C). Following solution heat treatment, the bars were given a "psuedo-coat" heat treatment of 1050°C for 4 hrs followed by a low temperature age of 800°C for 16 hours. Single edge notch crack growth rate specimens were machined from the heat treated bars. Both pin loaded (rotation permitted) and threaded specimens were created. Specimen notches were oriented to produce cracking along <010> crystallographic direction. Tests were conducted in load control mode using a servohydraulic test frame with the temperature controller of the induction furnace built into the feedback loop. Crack length measurements were obtained using potential drop methods at the maximum stress-minimum temperature waveform endpoint for each cycle. R-ratios ($\Delta K_{min} / \Delta K_{max}$) of 0.05 and -1 were applied. Crack growth rate measurements were obtained using increasing, decreasing, and constant K testing using computer algorithms for controlling the servohydraulic feedback loop as the crack length changes.

Fatigue cracks are observed to propagate normal to the direction of applied stress, however overload fractures are highly crystallographic. Figure 8 presents the experimentally derived models for the average crack growth rate of CMSX-3 for triangle out-of-phase wave form for the two R-ratios experimentally evaluated. The R-ratio (or mean stress) is observed to have a strong influence on the slope of the crack growth rate curve for this alloy. Such effects are related to the differences in the effective ΔK actually applied to the crack tip as a result of anticipated crack closure mechanisms [7] resulting from the differences in mean stress (plastic wake effect) and the influence of crack surface oxidation (figure 4).

MODELING AND PREDICTIONS

Using the experimentally collected data a waveform specific crack growth law for the superalloy can now be constructed. This is accomplished using performance information for the turbine operating conditions anticipated to occur during the mission profile (gas temperatures and pressures). Component thermal-mechanical fatigue driving forces are estimated using 3-D transient heat transfer and stress analysis of the component (Figure 9). Initial estimates are provided assuming thermo-elastic constitutive behavior which can be further refined using time dependent viscoplastic constitutive equations for localized regions of interest [8]. Using such analytical tools it is possible

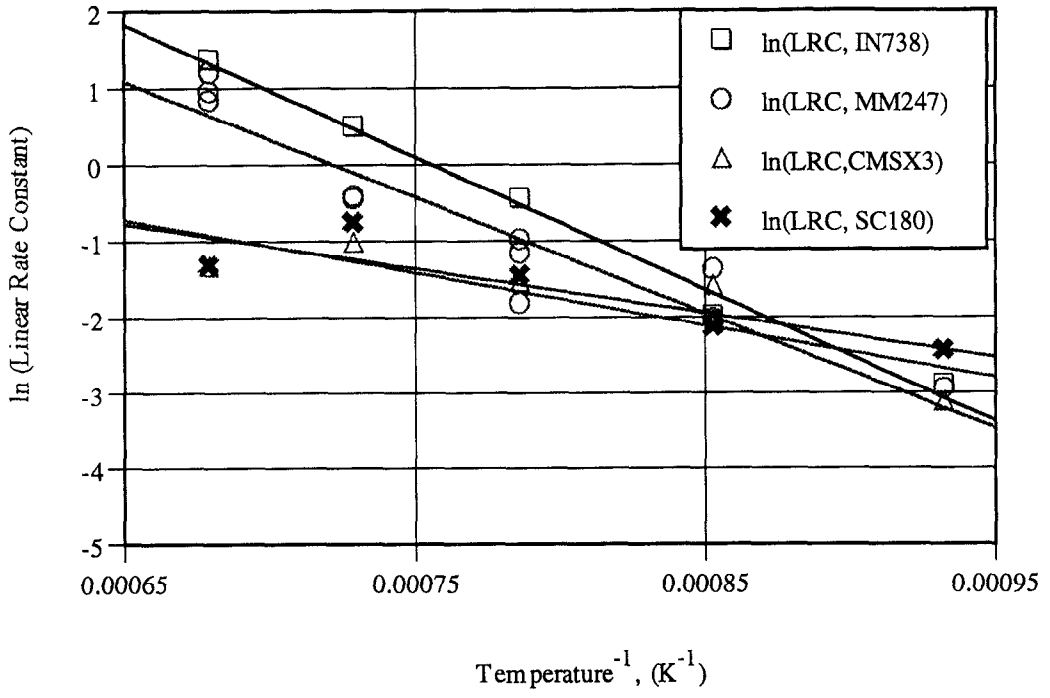

a.

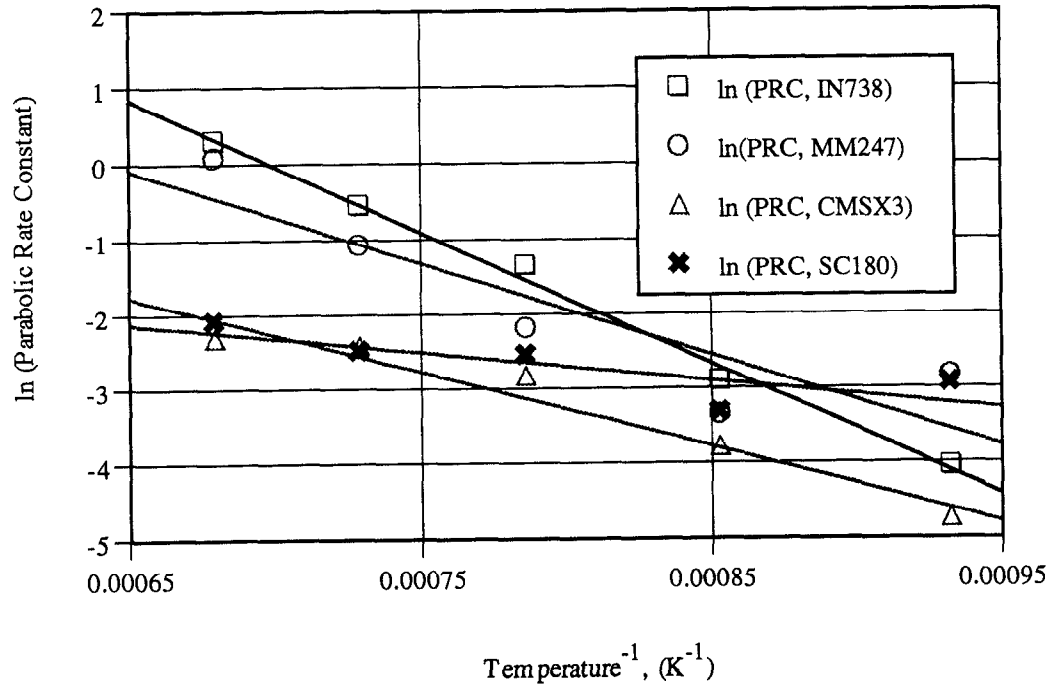

b.

Figure 7. Graphical Arrenhius-type description of the experimental data used for determination of a). Linear (Transient) and b). Parabolic (Steady State) rate constants for the superalloys listed within Table I when tested in stagnant air.

to define the maximum and minimum time/path dependent strain excursions experienced on the surfaces of the component during the anticipated gas turbine cycle. Using this information, the crack propagation life of the component is estimated by growing the crack analytically into the through-thickness component stress field along the anticipated crack path. For the specific case examined (gas generator turbine vane), the temperatures where the maximum and minimum stresses occur correspond closely to the experimentally measured TMF waveform (i.e. 538°–982°C). For this reason it was assumed that the mechanical crack growth resistance of the CMSX-3 superalloy

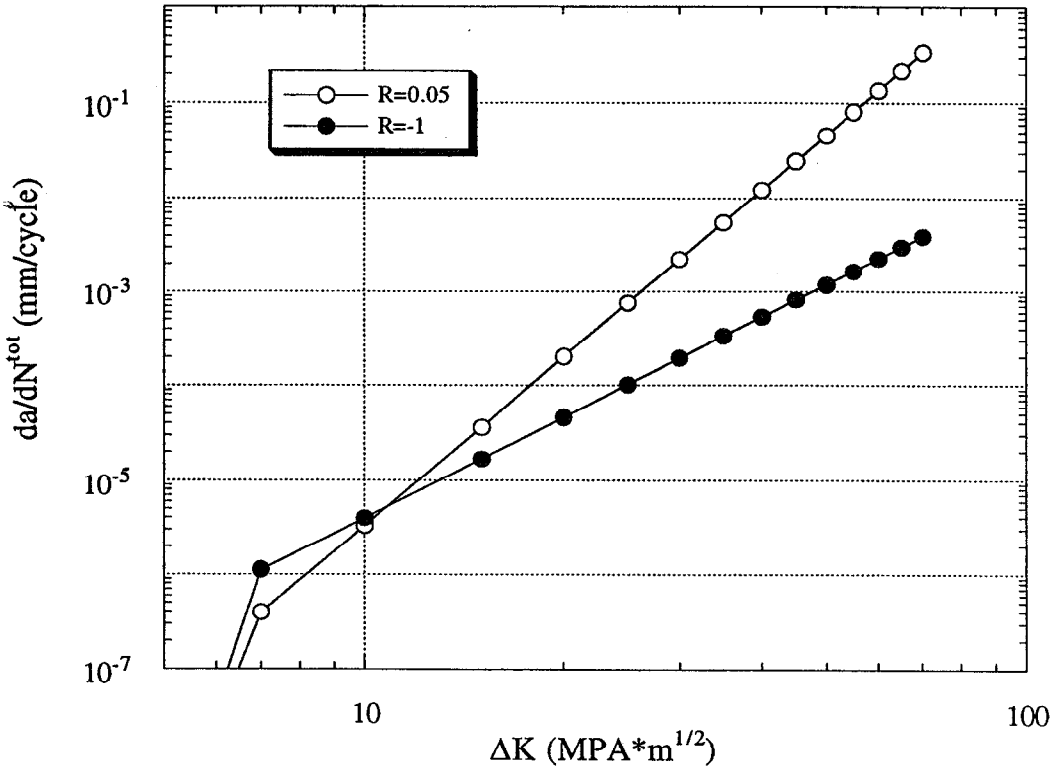

Figure 8. Experimentally derived models for the average TMF crack growth rate of CMSX-3 superalloy for triangle out-of-phase waveform cycling between temperatures of 538°C-982° C.

component during the vane TMF cycle can be represented by the experimentally measured TMF crack growth behavior (Figure 8). The effect of R-ratio changes during crack growth into the component are evaluated by interpolation between the two different crack growth curves at R=0.05 and R=-1. Environmental crack growth rates for the mission profile are determined based upon knowledge of the gas temperatures and pressures for the various mission cycle points. From this information it is possible to calculate the environmental crack growth increment

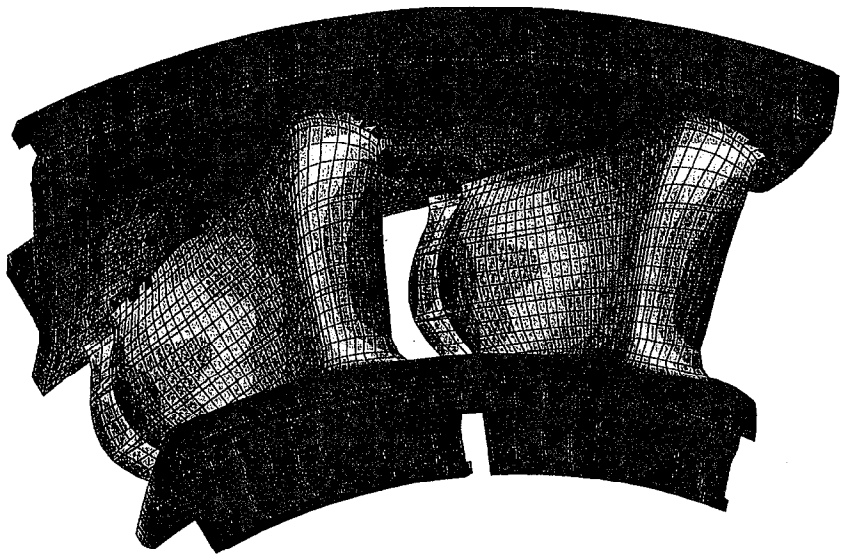

Figure 9. Three dimensional model of vane airfoil component employed to evaluate thermal and mechanical driving forces for TMF crack growth resistance of superalloy for a specific mission profile.

Table II. Comparison of mechanical and environmental crack growth rate of CMSX-3 for the laboratory and gas turbine engine environment for a short crack (0.07 mm) and a long crack (7.62 mm). All crack growth rates in mm/cycle.

Environment and waveform	Mechanical		Environmental
	0.07 mm crack	7.62 mm crack	both crack sizes
Laboratory Stagnant Air, 2.5 min dwell at 1 atm			
538C-982C OP TMF	1.8796E-07	4.1910E-04	3.2766E-10
Engine, 2.5 min dwell at 10 atm			
538C-982C OP TMF	9.40E-08	1.2903E-04	1.5037E-06

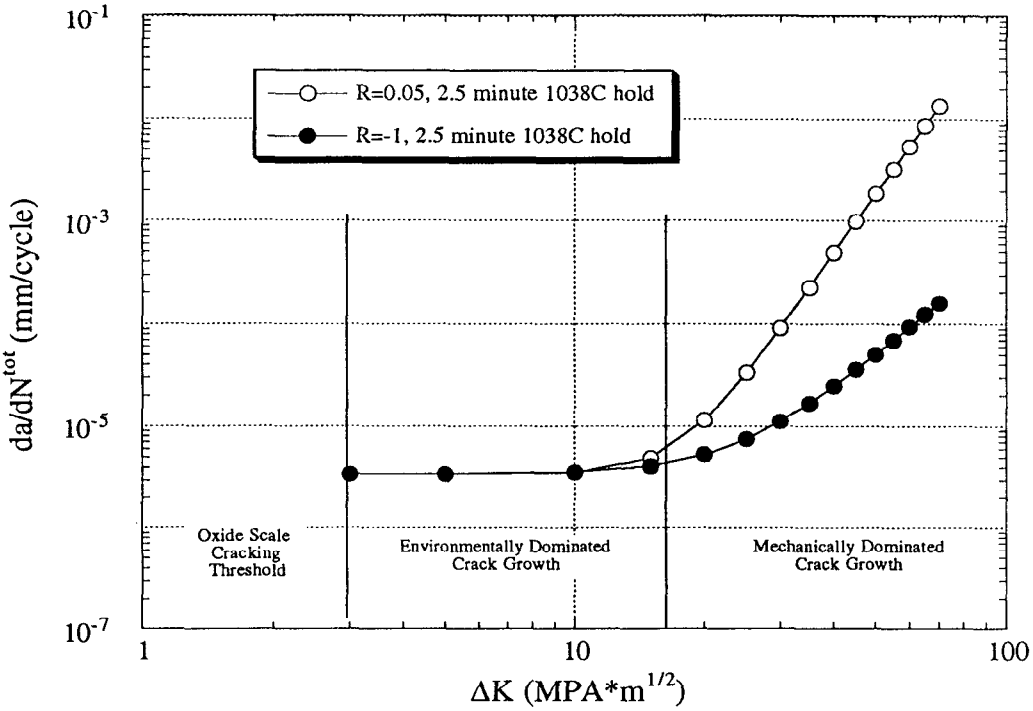

Figure10. Predicted crack growth resistance for CMSX-3 superalloy vane for 538°C-982°C out-of-phase TMF engine cycle with a 2.5 minute dwell at maximum power.

per engine cycle. This calculated crack growth increment is linearly added to the mechanical crack growth rate to predict the superalloy crack growth resistance for the specific component operating conditions (Figure 10):

$$da/dN_{Total} = da/dN_{env} + da/dN_{mech} \quad (3)$$

Use of the above described methodology to predict the damage observed within vane component after various engine tests is found to successfully predict the measured crack depths within a factor of two. As such the model is deemed to be acceptable for engineering purposes.

An example of the predictive capabilities of this TMF component lifing methodology will demonstrate the importance of considering the environmental contribution to crack growth. Table II indicates the predicted mechanical and environmental crack growth rates for two different crack depths in both ambient air and high pressure turbine environments. From this comparison it can be observed that environmental crack growth only becomes significant only for small crack depths in the turbine environment. As the crack grows further (for a uniform stress field), the contribution of the environment to the total crack growth becomes insignificant. Further examination of Table II reveals that the environmental crack growth rate predicted to occur during ambient pressure high temperature crack growth rate testing is insignificant as compared to that predicted to occur within the high temperature/high pressure gas turbine engine environment. For these reasons, use of superalloy crack growth rate data obtained in ambient air without correcting for environmental influences can lead to significant over-estimates of component propagation life (Figure 11). These comparisons indicate that the use of superalloy TMF crack growth resistance data obtained entirely from laboratory experiments conducted in ambient pressure may grossly underestimate the true crack growth

behavior within the gas turbine environment.

SUMMARY AND CONCLUSIONS

This paper has presented experimental and analytical methods for the estimation of superalloy crack growth resistance for out-of-phase TMF cycling experienced by gas turbine airfoils during engine cycling. The model uses experimentally derived estimates of crack tip transient and steady state oxidation to predict the amount of superalloy transferred into oxide ahead of a growing TMF fatigue crack. When combined with experimentally measured crack growth rates obtained from laboratory cycling, an analytical procedure was established for estimation of the crack growth resistance for the specific operating conditions under examination. This procedure is combined with previously presented methods for the prediction of coating induced crack initiation to estimate component TMF life for a specific mission profile. Use of these procedures for the prediction of TMF induced damage within superalloy gas turbine components of acceptable accuracy (factor of 2).

REFERENCES

[1] T.E. Strangman, "Thermal-Mechanical Fatigue Life Model for Coated Superalloy Turbine Component", Superalloys 1992, ed by S.D. Antolovich, R.W. Stusrud, R.A. MacKay, D.L. Anton, T. Khan, R.D. Kissinger, and D.L. Klarstrom, (The Minerals, Metals & Materials Society, Warrendale, PA, 1992), 795-804.

[2] H.L. Bernstein and J.M. Allen, "Analysis of Cracked Turbine Blades", Journal of Engineering for Gas Turbines and Power, 114 (1992), 293-301.

[3] M.I. Wood and G.F. Harrison, "Modelling the Deformation of Coated Superalloys under Thermal Shock", (Paper presented at the ASM Conference on Life Assessment and Repair Technology for Combustion Hot Section Components, Phoenix AZ, 1990).

[4] J. E. Heine, J.R. Warren, B.A. Cowles, "Thermal Mechanical Fatigue of Coated Blade Material" Final Report WRDC-TR-89-4027 under Contract F33615-89-C-5027, 1989.

[5] I. Linask and J. Dierberger, "A Fracture Mechanics Approach to Turbine Airfoil Design", ASME Paper No. 75-GT-79, 1975.

[6] S. Floreen and R. Raj, " Environmental Effects in Nickel-Base Alloys" Flow and Fracture at Elevated Temperatures, ed. by R. Raj, (The American Society for Metals, Metals Park Ohio, 1985), 383-405.

[7] H.L. Ewalds and R.J.H. Wanhill, Fracture Mechanics, (Edward Arnold Ltd, London, U.K. 1984), pp. 174-177.

[8] R.D. Krieg, J.C. Swearengen, W.B. Jones, "A Physically Based Internal Variable Model for Rate Dependent Plasticity", Unified Constituitive Equations for Creep and Plasticity ed by A. K. Miller, (Elsevier Applied Science, 1987).

ACKNOWLEDGEMENTS

Partial funding of this development was provided by the U.S. Army T800 engine program. The efforts of Mr. Chris Desidier, Mr. Harry Eckstrom and Mr. Dennis Chamblee of the AE materials test laboratory are gratefully acknowledged. All casting used thoughout this study were procurred from the Howmet Whitehall Casting Division, Whitehall, MI.

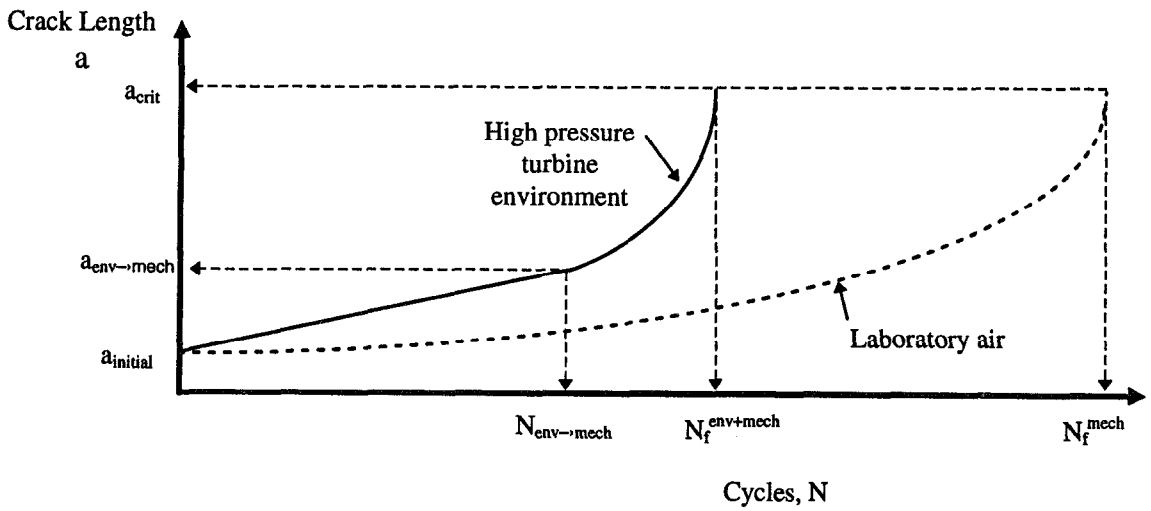

Figure 11. Comparison of crack growth rate behavior in laboratory air and the gas turbine environment.